Molecular Cell, Vol. 9, 1031–1044, May, 2002, Copyright ©2002 by Cell Press

c-Myc Can Induce DNA Damage, Increase Reactive Oxygen Species, and Mitigate p53 Function: A Mechanism for Oncogene-Induced Genetic Instability

Omid Vafa,[1] Mark Wade,[1] Suzanne Kern,[2] Michelle Beeche,[1] Tej K. Pandita,[3] Garret M. Hampton,[2] and Geoffrey M. Wahl[1,4]
[1]The Salk Institute for Biological Studies
La Jolla, California 92037
[2]Genomics Institute of the Novartis Research Foundation
San Diego, California 92121
[3]Center for Radiological Research
Columbia University
New York, New York 10032

Summary

Oncogene overexpression activates p53 by a mechanism posited to involve uncharacterized hyperproliferative signals. We determined whether such signals produce metabolic perturbations that generate DNA damage, a known p53 inducer. Biochemical, cytological, cell cycle, and global gene expression analyses revealed that brief c-Myc activation can induce DNA damage prior to S phase in normal human fibroblasts. Damage correlated with induction of reactive oxygen species (ROS) without induction of apoptosis. Deregulated c-Myc partially disabled the p53-mediated DNA damage response, enabling cells with damaged genomes to enter the cycle, resulting in poor clonogenic survival. An antioxidant reduced ROS, decreased DNA damage and p53 activation, and improved survival. We propose that oncogene activation can induce DNA damage and override damage controls, thereby accelerating tumor progression via genetic instability.

Introduction

The high fidelity of DNA replication and segregation characteristic of normal cells is often compromised in cancer cells. This can lead to genomic instability, a hallmark of neoplasia. Mutations in components of the cellular machinery that ensures faithful DNA replication, corrects errors, and regulates cell cycle progression have now been described in cancer predisposition syndromes (Bell et al., 1999; Chen et al., 1999; Fishel et al., 1993; Hwang et al., 1999; Leach et al., 1993) and in sporadic tumors (Ko and Prives, 1996; Wahl et al., 1997). These observations support models predicting that lesions engendering mutator phenotypes play an important role in cancer progression (Loeb, 2001).

One important pathway that impacts genetic stability involves the p53 tumor suppressor gene (Livingstone et al., 1992; Yin et al., 1992). p53 is a transcriptional regulator (el-Deiry et al., 1992; Jimenez et al., 2000; Kern et al., 1991) that plays a central role in cellular responses to various types of DNA damage (Kastan et al., 1992), hypoxia (Graeber et al., 1994), ribonucleotide depletion (Linke et al., 1996), and activation of cellular oncogenes such as *c-myc* (Zindy et al., 1998) and *ras* (Serrano et al., 1997). Activation of this pathway in normal cells results in cell cycle arrest, apoptosis, or premature senescence (Di Leonardo et al., 1994; Linke et al., 1996; Serrano et al., 1997; Hermeking and Eick, 1994). In addition, p53 is involved in a process during S phase that limits chromosome breakage when normal cells are exposed to agents that affect replication fork progression (Agarwal et al., 1998), and it can contribute to the G2 DNA damage response (Agarwal et al., 1995; Hermeking et al., 1997). Disabling the p53 pathway enables cells to enter and proceed through the cell cycle under conditions that increase the frequencies of aneuploidy and large-scale chromosomal structural alterations such as gene amplification, deletion, and translocation (Livingstone et al., 1992; Wahl et al., 1997; Yin et al., 1992). Inactivation of the p53-dependent apoptotic response and the increases in genetic instability that accompany loss of the p53 pathway are highly selected during cancer progression (Hollstein et al., 1991).

In light of the impact of p53 on apoptosis and chromosomal integrity, the modest effects of p53 deletion on development are surprising (Harvey et al., 1993; Sah et al., 1995). This may be explained by p53 deficiency alone being insufficient for induction of genetic instability. Consistent with this proposal, p53-deficient human cells underwent gene amplification only after they were exposed to clastogenic agents capable of initiating amplicon formation (Paulson et al., 1998; Poupon et al., 1994).

If genotoxic exposure is required for p53-deficient cells to acquire chromosomal abnormalities, what explains the genetic instability evident in tumor cells that have not been exposed to clastogens? Telomeric attrition can generate complex nonreciprocal chromosomal translocations through fusion-bridge breakage cycles (Artandi et al., 2000). Alternatively, mutations that precede p53 inactivation such as those that activate oncogenes might create a genome-destabilizing environment that also selects for loss of p53 function (Eischen et al., 1999). Several observations are compatible with this proposal. For example, ras overexpression induces premature senescence in normal cells by a mechanism involving p53 and the cyclin-dependent kinase inhibitors p21 (a p53 target) and $p16^{INK4a}$ (Serrano et al., 1997). ARF, a protein that is produced from an alternative reading frame transcript of the *$p16^{INK4a}$* gene, inhibits the function of the p53 negative regulator, MDM2 (Kamijo et al., 1997). Activated oncogenes can induce ARF and contribute to premature senescence (Sherr and Weber, 2000) by a mechanism proposed to involve "hyperproliferative signals" awaiting biochemical elucidation (Sherr and Weber, 2000). One clue to the nature of such signals derives from the striking similarity of the requirements for p53, p21, and p16 for oncogene and DNA damage-induced premature senescence (Di Leonardo et al., 1994; Robles and Adami, 1998; Sherr, 1998). Thus, it is possible that oncogene-induced arrest may derive, at least in part, from changes in gene expression that produce biochemical intermediates that induce DNA damage. This proposal is consistent with previous studies

[4]Correspondence: wahl@salk.edu

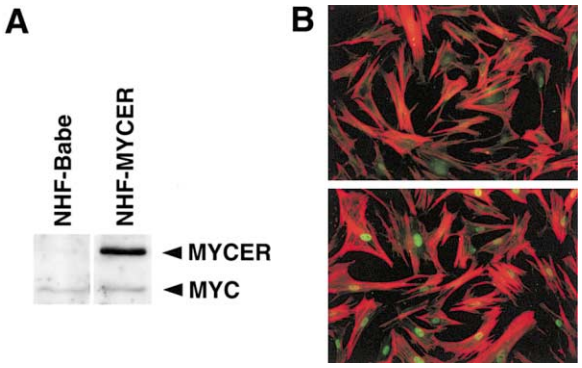

Figure 1. c-MycER Expression and Localization in NHF-MycER

(A) Cell lysates from NHF-MycER and NHF-BABE were analyzed by Western blot using anti-c-Myc monoclonal antibodies to detect both endogenous c-Myc and c-MycER protein. c-Myc and c-MycER are distinguished by the higher molecular weight of c-MycER fusion protein.

(B) Immunofluorescence microscopy of c-MycER. c-MycER was visualized in NHF-MycER cells in the absence or presence of ligand (top and lower panels, respectively) using anti-Myc monoclonal antibodies and FITC-conjugated secondary antibodies. c-MycER rapidly (<30 min) accumulates in the nucleus after ligand addition. Actin was detected using Texas red-X phalloidin.

reporting that activated c-Myc and ras can induce chromosome breakage and increase the frequency of gene amplification (Denko et al., 1994; Felsher and Bishop, 1999; Mai et al., 1996).

The studies reported here investigate whether oncogene activation induces DNA damage indirectly through cell cycle entry and progression under inappropriate conditions (Felsher and Bishop, 1999) or whether brief exposure to elevated oncogene levels engenders metabolic changes that create DNA lesions even in resting cells. Our data provide evidence that c-Myc overexpression can induce DNA damage, at least in part through the generation of oxidative stress. We further show that c-Myc activation can compromise the damage-sensing mechanism of normal cells. These combined effects of c-Myc could fuel genome destabilization and accelerate multistage tumor progression.

Results

Molecular Consequences of Activating c-MycER in Normal Human Fibroblasts

We determined whether c-Myc expression induces DNA damage using normal human fibroblasts with an inducible c-Myc transgene (NHF-MycER). These cells express a c-Myc protein fused to the ligand binding domain of the estrogen receptor (MycER) at levels approximately 5- to 10-fold higher than the endogenous c-Myc and comparable to those found in many human cancers and cell lines (Figure 1A). The fusion protein is inactive until estrogen (E2) or tamoxifen (OHT) is added to the medium, which results in the rapid translocation (i.e., <30 min) of a majority of the fusion protein to the nuclei of more than 95% of the cells in the population (Figure 1B). The transcriptional and functional capacity of the c-MycER transgene was tested using microarray analysis (Figure 2). Temporal patterns of c-MycER-induced expression relative to untreated control cells are depicted by hierarchical clustering. Noteworthy among this set of genes was the activation or repression of known c-Myc target genes (e.g., ornithine decarboxylase [ODC], prothymosin α [PTMA], cyclin D2, and gas-1), as well as many others that have recently been reported (e.g., fibrillarin and TRAP-1; Coller et al., 2000). Consistent with previous reports, c-Myc activated the expression of genes involved in multiple physiological functions, including basal metabolism, nucleotide biosynthesis, control of cell cycle progression, and apoptosis (Coller et al., 2000; Dang, 1999; O'Hagan et al., 2000; Packham and Cleveland, 1994).

Development of an In Situ Method to Detect and Quantify DNA Damage in Resting Cells

c-Myc expression in cycling cells can lead to chromosomal abnormalities (Felsher and Bishop, 1999; Mai et al., 1996). The following studies were designed to determine whether this is an indirect effect of deregulated c-Myc expression in cells traversing S phase or whether the biochemical consequences of its overexpression could produce DNA damage in resting cells.

We developed a sensitive method that combines terminal deoxynucleotidyl transferase (TdT)-mediated nick end labeling (TUNEL [Gavrieli et al., 1992]) with fluorescein-labeled nucleotides and deconvolution microscopy to visualize damaged nuclear DNA in G0/G1 cells. The observed TUNEL foci represent sites of DNA damage since they colocalize with proteins involved in DNA damage signaling or repair following γ irradiation (Figure 3A). A majority of TUNEL foci reacted strongly with antibodies selective for hMre11 and p95 which, together with Rad 50, comprise a complex that targets DNA damage for repair (Figure 3A; Nelms et al., 1998). Similar to hMre11, the TUNEL foci also colocalized as early as 10 min after γ irradiation with RPA-70 (data not shown) and with phosphorylated histone H2AX, which is rapidly phosphorylated at serine 139 following induction of double-strand breaks by γ irradiation (Figure 3B; Rogakou et al., 1998). By contrast, other proteins such as p53 and BRCA1 did not colocalize (within 10 min) with TUNEL signals in damaged G0/G1 arrested cells (Figure 3C), indicating that the colocalization of TUNEL with damage response proteins is not due to fortuitous overlap of the fluorescence signals.

We observed a direct correlation between the number of TUNEL/H2AX foci and the dose of irradiation (Figure 3D) and detected approximately 15–20 foci/Gy. The TUNEL signals were derived from induced DNA damage as unirradiated cells exhibited no or very few foci (1–5/nucleus; Figure 3). As 1 Gy γ irradiation should result in 20–40 double-strand breaks (DSBs) (Ward, 1990), we infer that the number of TUNEL foci that colocalize with damage response proteins provides a specific and reasonably accurate estimate of DSBs in resting cells. However, we note that 80–140 total TUNEL foci were detected in cells exposed to 4 Gy, suggesting that the TUNEL may detect some types of DNA damage to which the repair proteins do not localize or that the time interval allowed for damage protein localization to these foci may have been insufficient for maximal association.

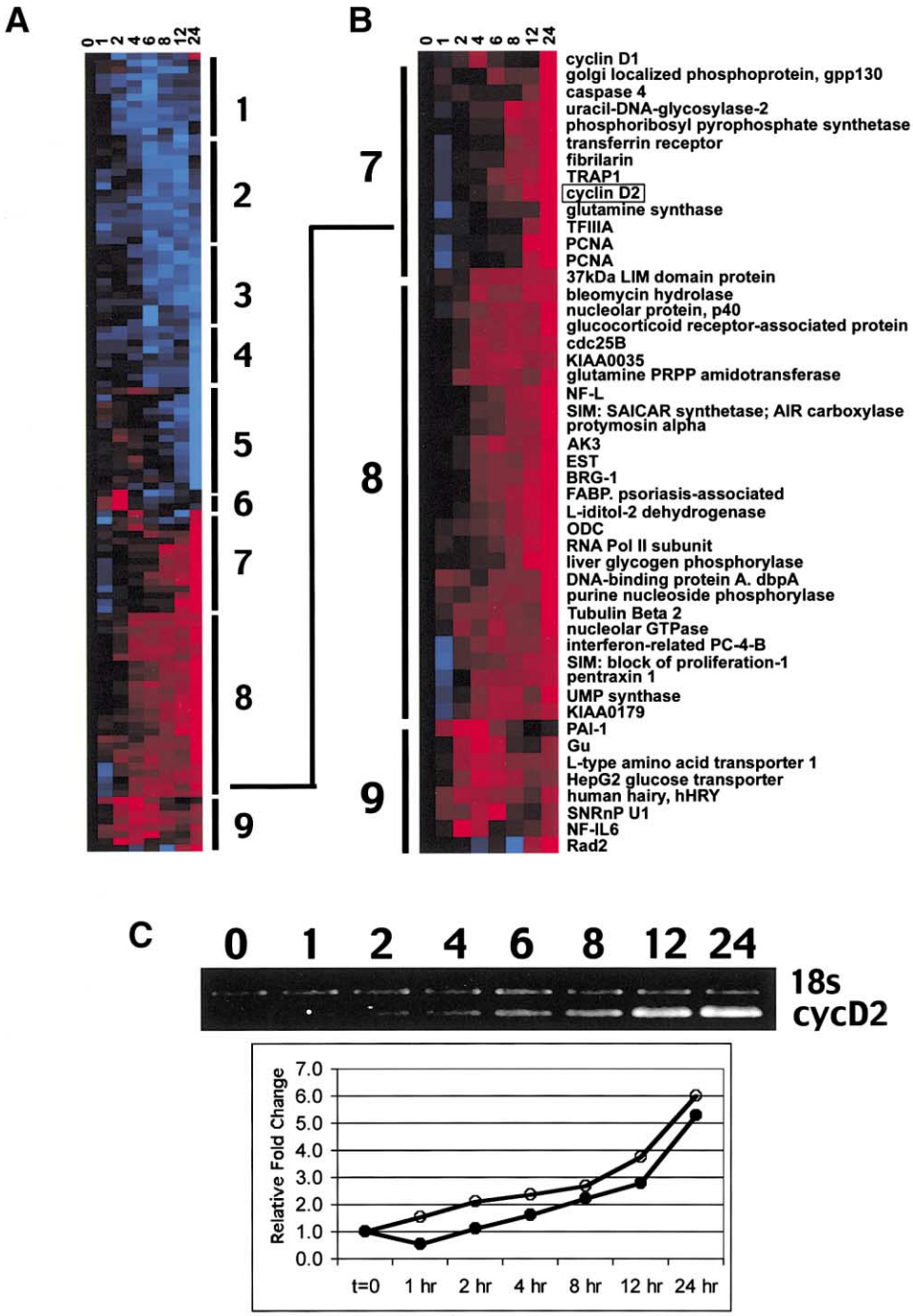

Figure 2. Temporal Patterns of Gene Expression following Induction of c-MycER in Serum-Starved Human Fibroblasts

(A) Total RNA from serum-starved, untreated NHF-MycER cells (t = 0) and NHF-MycER cells exposed to 17-β-estradiol for between 1 and 24 hr were hybridized on Affymetrix Hu6800 oligonucleotide GeneChips (see Experimental Procedures). Criteria (see Supplemental Data at http://www.molecule.org/cgi/content/full/9/5/1031/DC1) were used to identify 117 nonredundant genes exhibiting expression differences of at least 2-fold in one or more time points from replicate experiments. Relative fold differences in expression for 117 genes were transformed (LOG base2) and normalized. The "Cluster" software program developed by Eisen et al. (1998) was used to obtain a hierarchical view of fold changes in gene expression relative to untreated cells. Each row represents the normalized behavior of individual genes; each column represents "merged" replicate hybridization experiments from GeneChip arrays over a 24 hr period. Red boxes indicate relative increases in gene expression; blue boxes represent relative decreases in gene expression; black boxes represent values unchanged from control (t = 0) expression levels. Numbers to the right (1–9) represent approximate cluster boundaries delimiting different classes of behavior.

(B) An expanded view of the clusters representing upregulated genes (clusters 7–9).

(C) A representative example of semiquantitative RT-PCR validation of the array data using primers specific for cyclin D2. A 2% agarose gel with the products of a cycD2/18S rRNA multiplex reaction is shown in the top panel. The fold changes relative to t = 0 are shown for the array data (closed circles) and for the RT-PCR experiment (open circles).

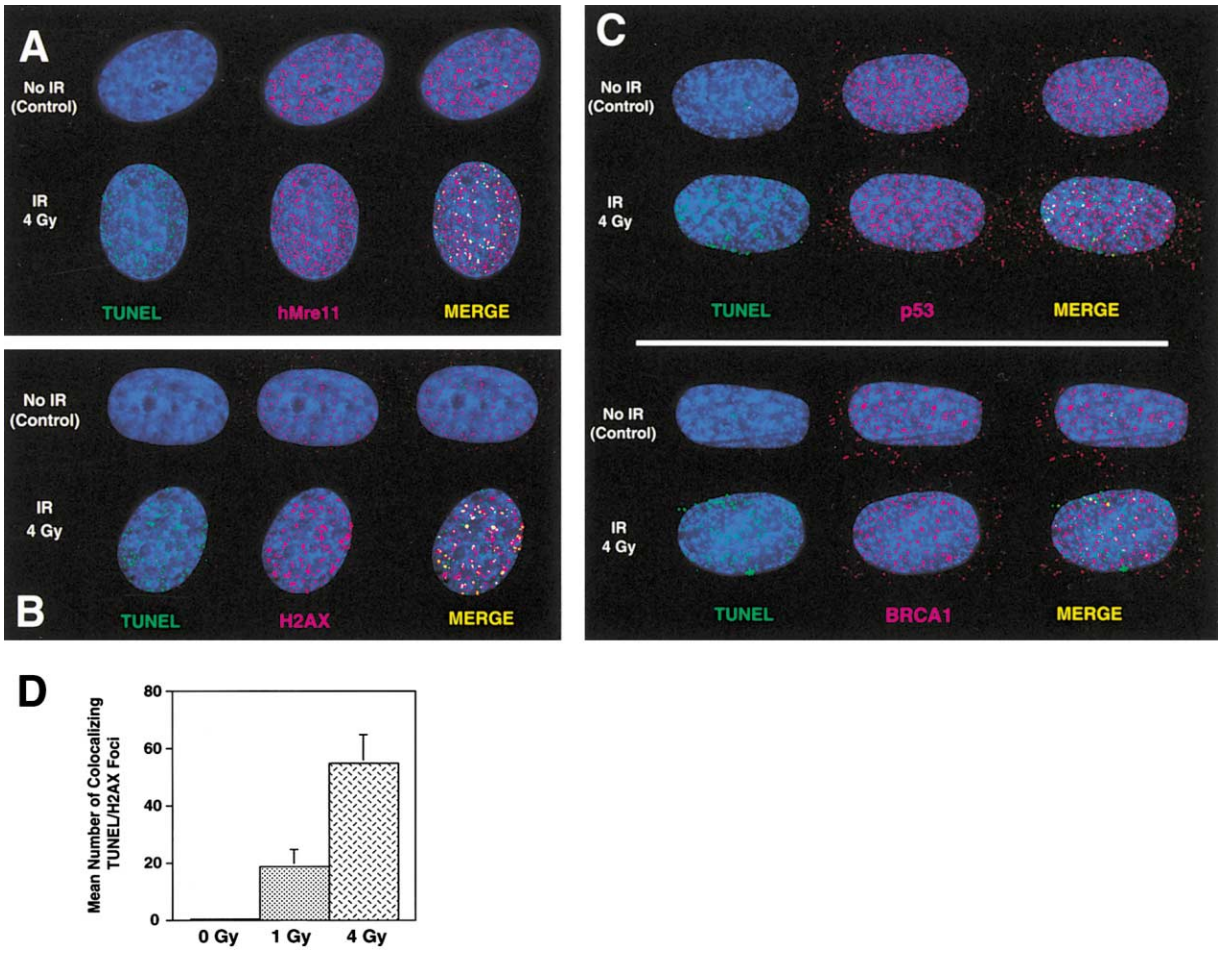

Figure 3. In Situ Detection of DNA Damage by Deconvolution Microscopy and TUNEL

Serum-deprived NHFs were irradiated (4 Gy) or mock irradiated, fixed after 10 min, labeled by TUNEL (green), and subsequently labeled with antibodies against hMre11 (A), H2AX (B), p53 and BRCA1 (C) (see Experimental Procedures), and their respective fluorophore-conjugated secondary antibodies (red, Cy3-conjugated anti-rabbit or anti-mouse). Note the high fraction of colocalizing foci (yellow) from TUNEL/hMre11 and TUNEL/H2AX merges in these representative nuclei and the relative absence of colocalization of TUNEL with p53 and BRCA1. The generation of colocalizing TUNEL/H2AX foci directly correlates to the dose of γ irradiation (D).

Deregulated c-Myc Activity Induces DNA Damage in G0 Cells

c-Myc overexpression can induce S phase entry of serum-deprived rodent and human cells (CHO, MCF-7, Rat1a, and NHF-MycER). However, fewer than 1% of the serum-deprived NHF-MycER cells entered S phase 8–9 hr after addition of OHT, and only 7%–8% entered S phase by 24 hr (data not shown). Consistent with these data, analysis of the kinetics of gene expression (Figure 2) showed that upregulation of genes involved in DNA synthesis or cell cycle progression such as PCNA and cycD2 was significant only after 8 hr of c-MycER activation and maximal at 12–24 hr. These increases in gene expression were paralleled by the decreased expression of negative regulators of S phase progression, such as gas-1 (a known c-Myc target [Lee et al., 1997]) and gas-3, which were minimal at 12–24 hr. Based on these data, we evaluated DNA damage in serum-starved cells induced for fewer than 8 hr so that more than 95% of the cells would still be in G0/G1, and therefore TUNEL-positive signals would be unlikely to result from S phase entry or progression.

Serum-deprived NHF-MycER were cultured with ligand (c-MycER activated) or without ligand (c-MycER inactive) for the indicated times and then doubly stained for TUNEL and hMre11 or p95. Very few (5%) uninduced NHF-MycER cells exhibited more than 10 TUNEL/hMre11 foci (the majority had 1–5 foci, Figure 4A). Ligand-treated NHF-BABE cells had very few ($<$5) colocalizing hMre11/TUNEL foci (Figure 4A). By contrast, the majority of induced NHF-MycER ($>$95%) had numerous foci as early as 4 hr after ligand addition (mean of 23 hMre11/TUNEL foci/nucleus with a range of 6 to 58) and increased to a mean of approximately 70 foci per cell by 8–9 hr after ligand addition (ranging from 20–125 foci/nucleus; Figure 4B). Thus, TUNEL/hMre11 foci were detected in cells with activated c-Myc well in advance of S phase entry. The ability of c-Myc to induce DNA damage was confirmed using premature chromosome condensation (PCC) technology (Johnson and Rao, 1970; Pandita et al., 1994). The background breakage frequency was approximately the same in both cell types (0.03 breaks/NHF-BABE cell; 0.06 breaks/NHF-MycER cell, Figure 4C). Ligand treatment did not induce chro-

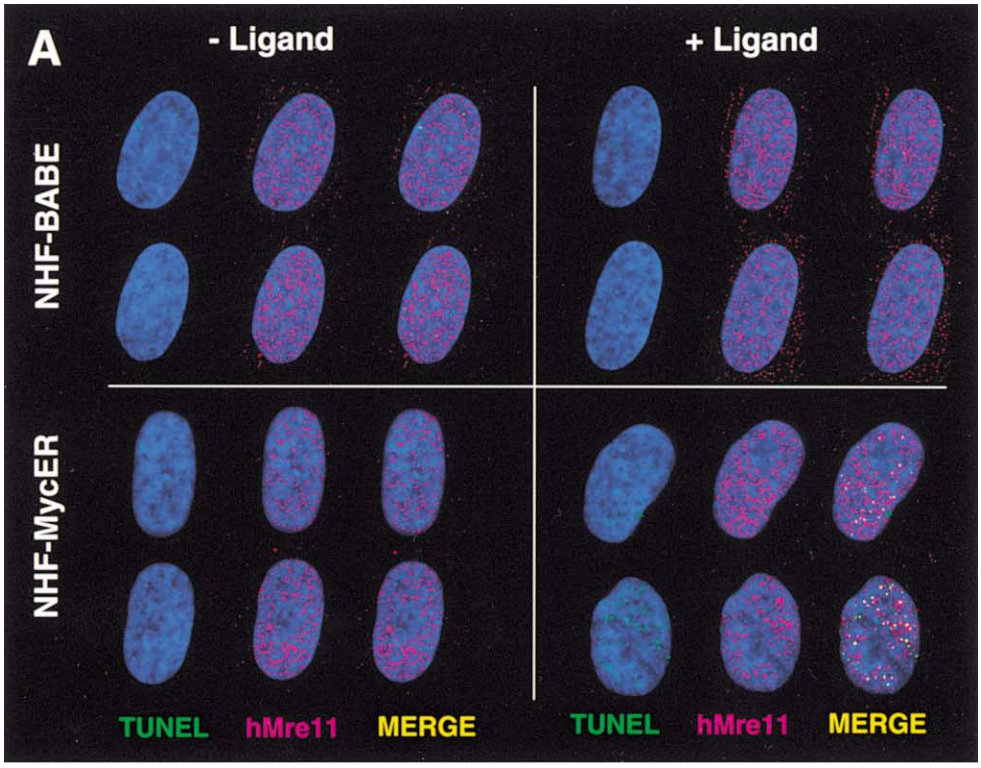

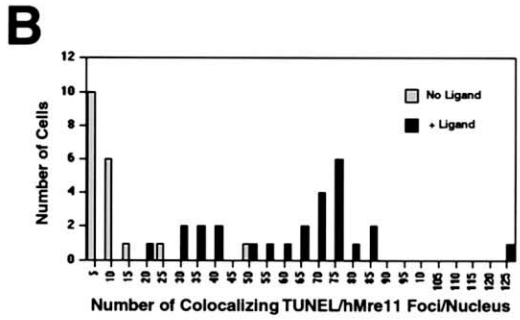

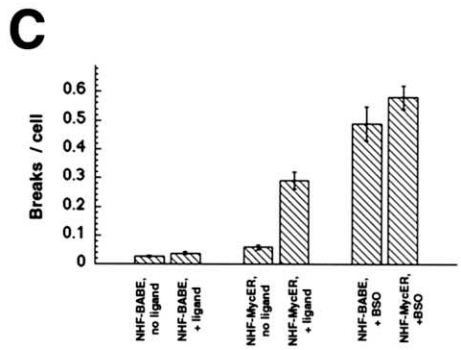

Figure 4. Myc Activation Induces DNA Damage in Serum-Deprived NHF-MycER

(A and B) NHF-MycER were serum deprived 48 hr, activated with ligand for 8.5 hr, and processed for TUNEL (green) and anti-hMre11 (red) before deconvolution microscopy. Note the generation of TUNEL foci that colocalize with hMre11 after c-MycER activation. The number of colocalizing foci per nucleus of 45 deconvolved nuclei before and after c-MycER activation is shown, which is representative of three separate experiments. Untreated NHF-BABE cells contained very few hMre11/TUNEL foci and did not exhibit an increase in foci after ligand addition (A).

(C) Chromosome damage in G0/G1 fibroblasts after 8.5 hr of c-MycER activation or BSO treatment was determined by PCC. Damage is plotted as breaks per cell with a minimum of 100 counts per treatment.

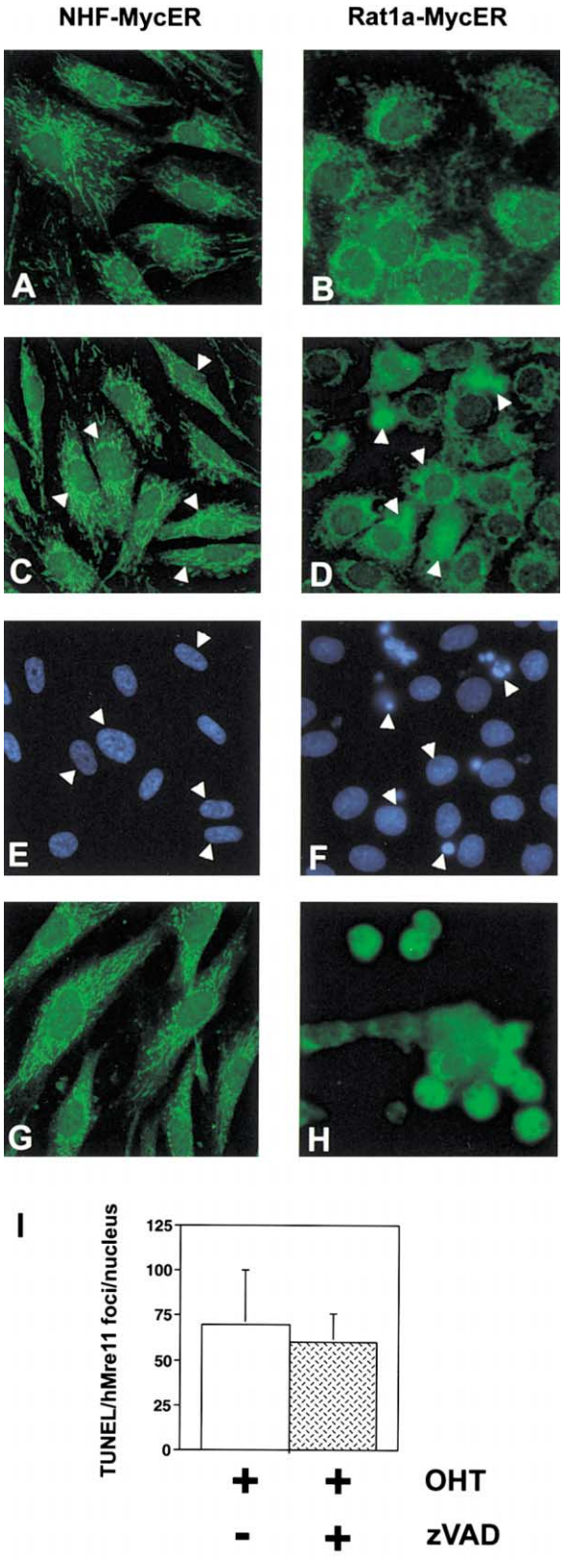

Figure 5. Release of Cytochrome *c* Is a Late Event following Activation of c-Myc in NHFs

NHF-MycER and Rat1a-MycER cells were serum starved for 48 hr prior to activation of c-Myc for 8 or 48 hr. After 8 hr, NHF-MycER cells retained a threadlike distribution of cytochrome *c* (green) and normal nuclear (blue) morphology ([C and E], arrowheads indicate the same cell). In contrast, Rat1a-MycER cells displayed diffuse cytochrome *c* staining in many cells which preceded or accompanied nuclear apoptosis ([D and F], arrowheads indicate the same cell). After 48 hr OHT treatment, cytochrome *c* distribution in NHF-MycER remained threadlike ([G], compare to untreated cells in [A]) but was diffuse in Rat1a-MycER ([H], compare to untreated cells in [B]). (I) Damage induction is not reduced by inhibition of caspases. NHF-MycER cells were pretreated for 1 hr with 100 μM zVAD.fmk and cultured in its presence during c-MycER activation for 8.5 hr. The number of colocalizing TUNEL/hMre11 foci was determined, and a control experiment in which zVAD.fmk was not included was performed in parallel.

mosome breakage in NHF-BABE cells but did produce a significant increase in the number of breaks in NHF-MycER cells (Figure 4C). We observed fewer DSBs using PCC than predicted from the TUNEL assay, but this is expected since PCC yields only one to three double-strand breaks per 1 Gy γ irradiation (Pandita and Hittelman, 1992). Taken together, these data indicate that active cell cycling is not required for induction of DNA damage by c-Myc. However, they do not exclude the possibility that additional DNA damage or exacerbation of damage generated in G0/G1 may result from aberrant cell cycle progression induced by expression of c-Myc at supraphysiologic levels (Felsher and Bishop, 1999).

Induction of DNA Damage in NHF-MycER Is Not Preceded by Measurable Apoptosis

Since c-Myc can induce apoptosis in rodent fibroblasts and human tumor cells deprived of survival factors (Evan et al., 1992; Hermeking and Eick, 1994), we determined whether the DNA damage foci reported above resulted from induction of apoptosis in NHF-MycER cells. c-Myc overexpression can destabilize the mitochondria in rodent cells, leading to cytochrome *c* release and caspase-associated endonuclease activity (Juin et al., 1999). Another mitochondrial protein, endonuclease G, is released concomitantly with cytochrome *c* and can induce DNA fragmentation independent of caspase activation (Li et al., 2001). However, we observed no evidence of cytochrome *c* release in serum-starved NHF-MycER cells treated with OHT for 8 or 48 hr (Figure 5). Dual staining with MitoTracker confirmed that cytochrome *c* colocalized with mitochondria (data not shown). In contrast, cytochrome *c* release in serum-starved Rat1a-MycER cells was detected 8 hr following addition of ligand and was observed in most cells by 48 hr (Figure 5). Furthermore, we did not observe other markers of apoptosis in activated NHF-MycER cells such as PARP cleavage, nuclear condensation, or annexin-V staining (data not shown).

The general caspase inhibitor zVAD.fmk prevents the DNA fragmentation associated with Myc-induced apoptosis (McCarthy et al., 1997). If the DNA lesions detected by TUNEL/hMre11 colocalization are downstream consequences of caspase activation, they should be reduced or eliminated by treatment with zVAD.fmk. However, zVAD.fmk treatment did not significantly reduce the number of TUNEL foci after Myc activation (Figure 5I). Taken together, these data reveal that c-Myc activation in NHF-MycER cells elicits DNA damage by

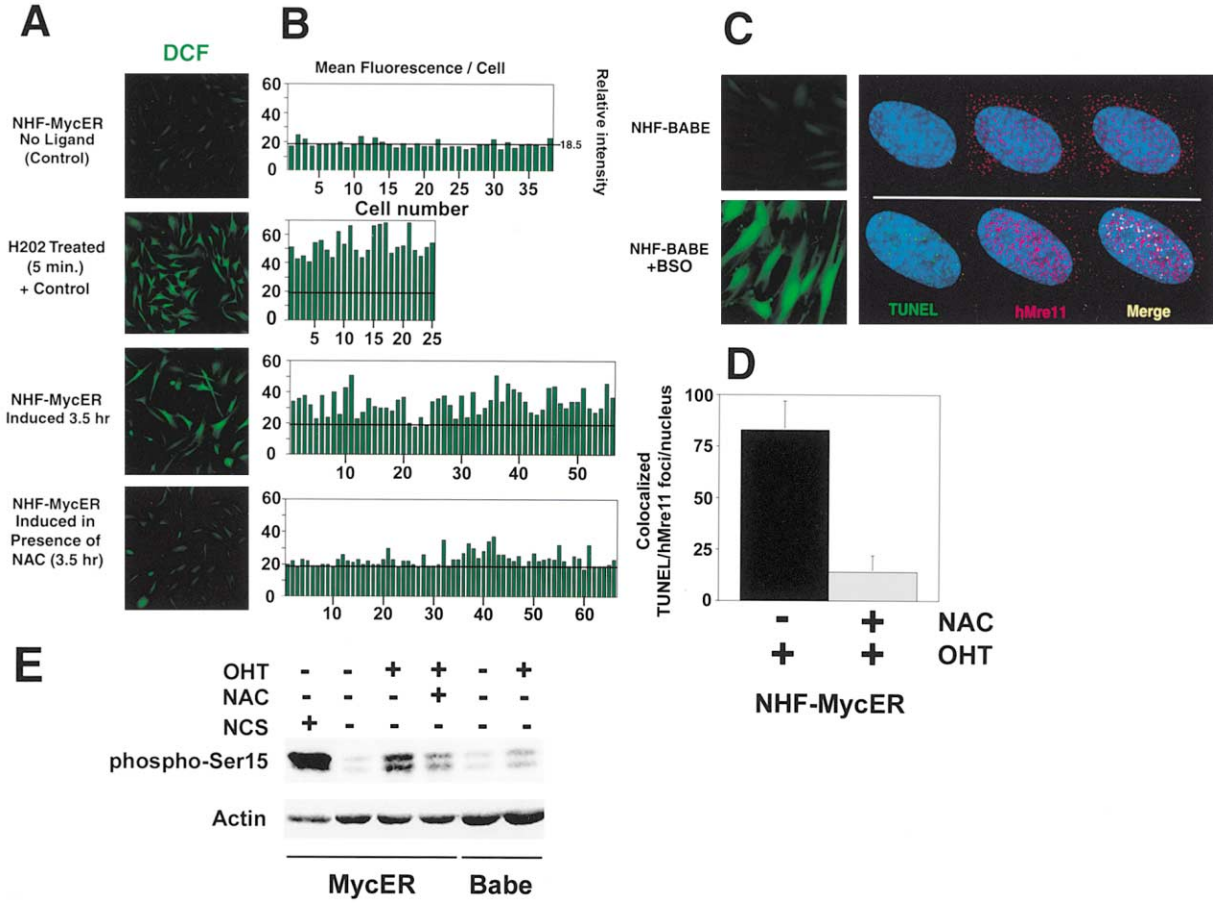

Figure 6. Correlation between c-MycER Induction of ROS and DNA Damage in G0/G1 Cells

(A–C) ROS levels in NHF-MycER and NHF-BABE were detected by a microscopic fluorescence assay using dichlorofluorescein diacetate (DCFDA) (Ohba et al., 1994). (B) Cellular mean fluorescence was quantified by digital image analysis using OpenLab software (OpenLab, Improvision, Coventry, England). Serum-deprived NHF-MycER cells were either uninduced or treated with 0.3% H_20_2 for 5 min (positive control) or preincubated with 5 mM NAC before c-Myc activation. (C) Serum-deprived NHF-BABE treated with BSO overnight (100 μM) exhibit elevated levels of ROS and DNA damage detectable by TUNEL signals in excess of TUNEL/hMre11 colocalization.

(D) NHF-MycER cultured in the presence or absence of 5 mM NAC for the last 24 hr of serum deprivation were evaluated for the number of damage foci per nucleus detectable as colocalized hMre11/TUNEL foci after 8 hr of MycER activation.

(E) NHF-MycER or NHF-BABE were serum starved for 48 hr in the presence (+) or absence (−) of NAC for the final 24 hr. For the following 8 hr, cells were either left untreated or treated with NAC and/or OHT before release into serum containing 10% dFBS. After 24 hr, protein lysates were analyzed by Western blotting for p53 phosphorylated at Ser15.

a mechanism that involves neither mitochondrial disruption and associated release of caspase-independent DNAases nor activation of a caspase-dependent process.

c-MycER Activation Elevates Reactive Oxygen Species, which Correlates with DNA Damage Induction and p53 Activation

Reactive metabolic intermediates, such as reactive oxygen species (ROS), can generate DNA damage directly or through activation of topoisomerase (Li et al., 1999). We therefore analyzed whether c-MycER activation elevated ROS levels in serum-deprived NHF-MycER cells. A significant increase in ROS was detected 3–4 hr after activation (Figure 6A) and persisted for at least 8 hr after c-Myc activation. Activated NHF-MycER cells exhibited at least two to three times the mean cellular fluorescence intensity of ligand-treated NHF-BABE or nonactivated NHF-MycER (Figure 6B). This level of ROS is similar to that produced by brief treatment with H_20_2 (Figure 6B).

DNA damage induces rapid phosphorylation of p53 on Ser15 by the damage-activated kinase ATM (Rotman and Shiloh, 1999). Activation of c-Myc in NHF-MycER cells increased p53 abundance (data not shown) and phosphorylation of Ser15 (Figure 6E), although the amount appeared to be somewhat lower than that elicited by treatment with the radiomimetic agent neocarzinostatin (NCS).

Antioxidants Reduce ROS and Can Limit the DNA Damage Induced by c-Myc

If the increased ROS generated by c-Myc activation causes DNA damage, then antioxidants should diminish ROS levels, limit damage induction by c-Myc, and reduce or prevent p53 activation. We tested these possi-

bilities by first determining whether the antioxidant N-acetyl-L-cysteine (NAC) can reduce ROS levels in cells with activated c-Myc. NAC significantly reduced ROS levels in the majority of cells with activated c-Myc (Figure 6A) and decreased by approximately 80% the amount of DNA damage generated by c-Myc activation (Figure 6D). Finally, exposing NHF-MycER to NAC prior to c-Myc activation significantly reduced the amount of p53 phosphorylated on Ser15 (Figure 6E). Importantly, expression array and semiquantitative RT-PCR showed that NAC did not significantly reduce expression of c-Myc activated genes using the specified conditions (data not shown).

These data raise the question of whether the increased ROS levels generated by c-Myc activation are sufficient to account for the induction of DNA damage. We evaluated the ability of ROS alone to generate DNA damage using buthionine-sulfoximine (BSO) to inhibit γ-glutamyl-cysteine synthetase, which increases ROS by depleting glutathione pools (Meister, 1983). A 24 hr treatment of quiescent NHF with BSO significantly and uniformly increased cellular ROS (Figure 6C) and generated numerous TUNEL/hMre11 foci (mean of 135 foci/nucleus) and chromosome breaks detectable by the PCC method (Figure 4C). Importantly, under the conditions of BSO treatment employed, we did not observe induction of apoptosis in these NHF. Taken together, these data are consistent with the proposal that c-Myc activation in NHF increases ROS levels, which induces DNA damage and elicits a DNA damage response involving p53.

Activation of c-Myc Compromises the DNA Damage Response

Ectopically expressed c-Myc in rodent cells can overcome growth arrests induced by activation of a temperature-sensitive p53 (Hermeking et al., 1995) or by a variety of conditions that lead to hypophosphorylated pRb and other pocket proteins (Alevizopoulos et al., 1997). These observations raised the possibility that c-Myc might also be able to overcome the p53-dependent arrest induced by DNA damage in NHF. We tested this possibility by examining the response of NHF-MycER cells to γ irradiation in the presence or absence of OHT. c-Myc activation induced 21% of the control cells to enter S phase by 24 hr after OHT addition (Figure 7A). More than 90% of the irradiated cells with inactive c-Myc (no OHT) remained arrested in G1, and only 1.2% entered S phase (Figure 7A). In contrast, 11.5% of NHF-MycER cells irradiated in the presence of activated Myc entered the cell cycle in the presence of substantial DNA damage (Figure 7A).

The cell cycle arrest response of NHF to ionizing radiation is largely if not entirely dependent on p53 (Kastan et al., 1991). Consistent with this, p53 levels increased substantially after c-Myc activation alone or in combination with irradiation (Figure 7B). As expected, pRb remained in its growth-suppressive, hypophosphorylated form subsequent to irradiation in control cells in the presence or absence of ligand as well as in NHF-MycER cells that were not treated with ligand (Figure 7B, compare lanes 2 and 4 to lane 6). Myc activation in irradiated cells appeared to increase modestly the ratio of hyper- to hypophosphorylated pRb (Figure 7B, compare lanes 6 and 8), but previous studies demonstrated that activated Myc could drive cells into cycle even if they had high levels of hypophosphorylated pRb (Alevizopoulos et al., 1997). Microarray analysis of irradiated NHF-MycER revealed upregulation of many p53 target genes (e.g., p21/WAF-1, gadd45, gadd153, APO-1) in the presence or absence of activated c-MycER as well as increases in expression of many established c-Myc target genes (e.g., cyclinD2). A sustained increase of the antiapoptotic gene, BAG-1, correlated with elevated levels of BAG-1 protein (Figure 7B). Moreover, Western analyses showed that Myc activation did not diminish p53 (Figure 7B) or p21 induction (data not shown). These data reveal that c-MycER activation compromises the DNA damage-induced arrest response in human cells, but the mechanism does not involve diminished p53 activation.

Activation of c-Myc Reduces Long-Term Cell Viability, but Antioxidants Mitigate Growth Inhibition

We used colony formation analyses to assess the long-term consequences of brief c-MycER activation. There was a significant reduction in colonies formed after c-MycER activation in NHF-MycER cells (Figure 7C). By contrast, OHT did not affect colony formation in NHF-BABE cells. These data show that brief activation of c-Myc in G0/G1 is sufficient to reduce the long-term viability of NHF. TUNEL analyses showed that preincubation with the antioxidant NAC reduced DNA damage induced by c-Myc (Figure 6D). To determine whether a reduction in DNA damage improved cell viability, we examined the effect of NAC pretreatment in the colony outgrowth assays. NHF-MycER cells treated only with OHT grew very sparsely, failed to form colonies, and exhibited a large, flat phenotype reminiscent of senescence (Figures 7D and 7E). In contrast, preincubation with NAC prior to treatment with OHT restored clonogenic capacity (evident as colonies of greater than 30 regular-sized cells, Figures 7D and 7E). Pretreatment with NAC also reduced the number of cells that were positive for senescence-associated β-galactosidase activity (data not shown). These results suggest that Myc induction of ROS may reduce long-term viability by inducing DNA damage, which subsequently activates a senescence program in NHF.

Discussion

c-Myc Activation in Resting Cells Generates DNA Damage Associated with Elevated ROS Levels

Activated oncogenes can transmit signals to p53 that result in senescence or apoptosis, but the biochemical basis of the signal has remained elusive. We now provide direct evidence that brief expression of c-Myc in resting cells generates sufficient ROS to produce DNA strand breaks, activate p53, and reduce clonogenicity.

Our data show that c-Myc-induced DNA damage occurred in the absence of apoptosis. These results agree with recent studies showing that human primary cells can suppress the ability of oncogenes to induce cell death (Duelli and Lazebnik, 2000). On the other hand, ROS production by activated c-Myc correlated strongly with induction of DNA damage. Furthermore, the antioxi-

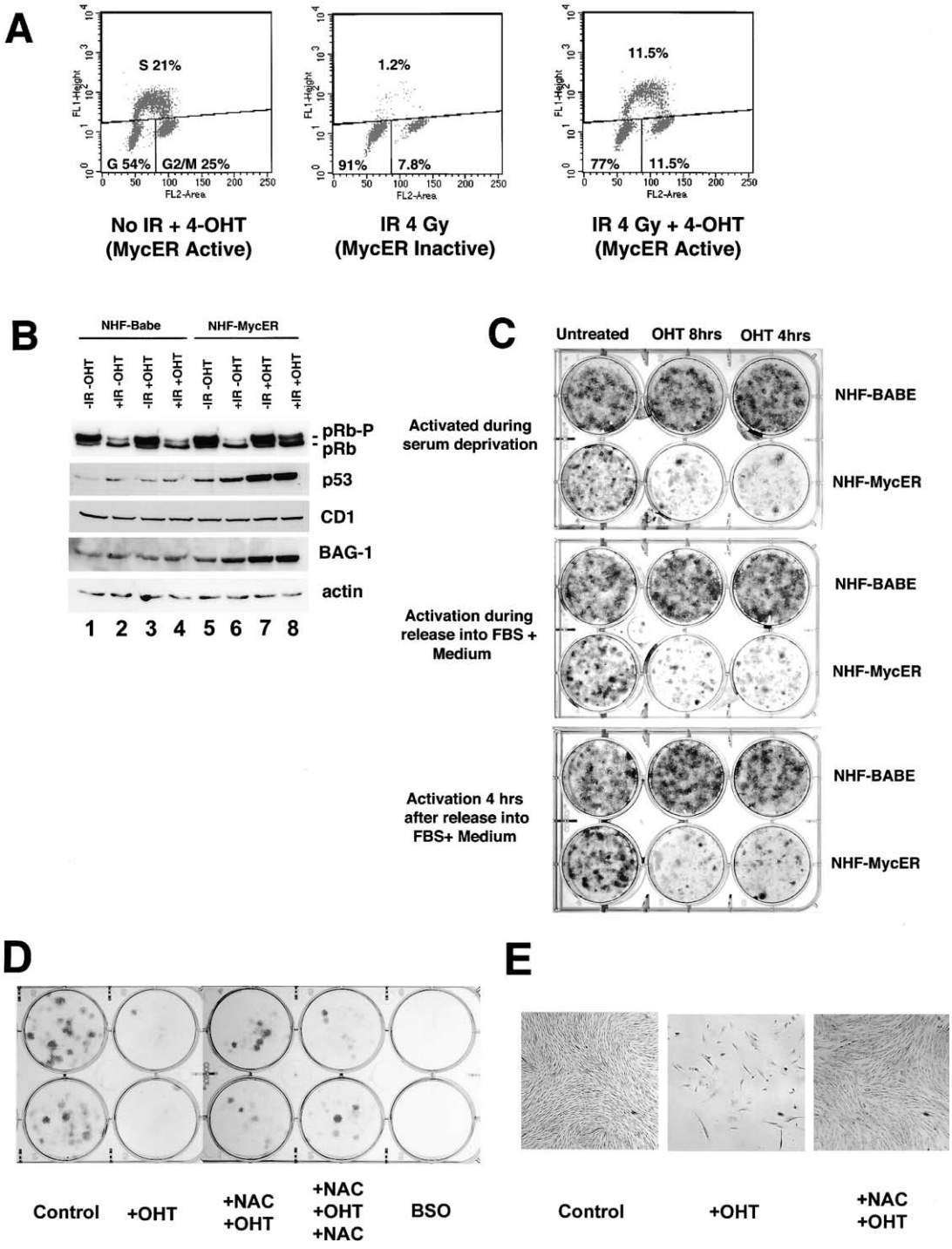

Figure 7. c-Myc Overrides the p53-Dependent G1 Arrest Induced by DNA Damage and Reduces Long-Term Cell Viability after Its Brief Activation

(A) NHF-MycER were synchronized by serum deprivation for 48 hr, released into media containing 10% dFBS for 4 hr, and then irradiated (4 Gy) or left untreated in the presence or absence of ligand. Cells were pulse labeled with BrdU for 1 hr at 24 hr after irradiation and processed for flow cytometric analysis. Percentages indicate the fraction of cells in each phase of the cell cycle.

(B) NHF-MycER and NHF-BABE were treated as in (A) and 24 hr after irradiation were analyzed for protein levels of Rb/Rbp, p53, cyclin D1, BAG-1, and actin.

(C) Cell viability assays by colony formation in NHF-MycER and NHF-BABE. c-MycER was activated under various growth conditions before washing off ligand and reculturing in growth medium for an additional 6 days. While brief c-MycER activation significantly reduced cell viability, pretreatment with NAC restored colony forming ability ([D]; [E] shows higher magnification of colonies). BSO treatment was included as a positive control for oxidative stress-induced suppression of colony outgrowth. These experiments were repeated at least twice, and representative results from each experiment are shown.

dant NAC, which does not prevent c-Myc-induced apoptosis in rodent fibroblasts (G. Evan, personal communication), produced an 80% decrease in the number of c-Myc-induced TUNEL/hMre11 signals and improved cell survival after c-Myc activation. Our studies also show that c-Myc activation produces the molecular hallmarks of a DNA damage response, including p53 accumulation and phosphorylation on Ser15. Ser15 is often phosphorylated after treatment with agents that induce DNA damage and has been linked to p53 stabilization and transcriptional activation (see Wahl and Carr, 2001, for a recent review). The reduction of Ser15 phosphorylation by NAC indicates that induction of this modification by activated c-Myc is at least partially due to ROS-mediated DNA damage. Other studies show that c-Myc-induced accumulation of p53 is partially dependent on ARF (Zindy et al., 1998) and probably involves transcriptional upregulation of ARF by E2F (Bates et al., 1998). Interestingly, recent data indicate that E2F can be activated by DNA damage (Lin et al., 2001), although it remains to be determined if ROS or ROS-induced damage activates E2F.

ROS Induction by Oncogenes

c-Myc could induce ROS by several mechanisms. c-Myc-mediated activation of p53 could lead to the activation of p53 target genes reported to be involved in oxidative metabolism and ROS production (Polyak et al., 1997). We do not favor this hypothesis, as c-Myc activation elevated ROS levels in E6-expressing NHF (data not shown). Another possibility is that ROS are generated by the activation of c-Myc target genes, such as ODC (Packham and Cleveland, 1994). However, we found that DFMO, a specific inhibitor of ODC, did not prevent the increase in ROS following Myc activation, nor did it reduce ROS in tumor cells with amplified c-Myc genes (data not shown). Nonetheless, it is clear that c-Myc regulates numerous genes involved in intermediary metabolism, and ROS may result from biochemical imbalances generated following unscheduled synthesis of many gene products (Dang, 1999). Since we observed that c-Myc induced ROS colocalized with mitochondria (O.V. and M.W., unpublished data), and prior studies show frequent mitochondrial DNA deletions in cells overexpressing c-Myc (Factor et al., 1998), it is possible that some of these biochemical imbalances may impinge on mitochondrial oxidative metabolism.

Excess ROS production may also result from the activation of other oncogenes involved in multiple signal transduction pathways in diverse cell types and is not likely to be limited to activation of c-MycER in fibroblasts. Hepatocytes in transgenic mice engineered to overexpress c-Myc also exhibited increased ROS which was increased further by TGF-α (Thorgeirsson et al., 2000). The ability of c-Myc alone to induce sufficient ROS to generate DNA damage may depend on cell type and genetic background. For example, no increase in DNA damage was noted in c-Myc-expressing hepatocytes, while c-Myc/TGF-α-expressing hepatocytes did manifest DNA damage (Thorgeirsson et al., 2000). Cell type-specific effects may also explain why c-Myc activation in hematologic malignancies is not usually associated with extensive chromosomal instability. Recent chromatin immunoprecipitation data also demonstrate that the complement of genes induced following activation of c-Myc is dependent on growth conditions (Frank et al., 2001). It is likely that the extracellular milieu, including oxygen tension (Lee et al., 1999), could influence the biochemical changes (i.e., ROS production) resulting from activation of c-Myc or other oncogenes.

Other oncogenes such as activated ras can also alter biochemical pathways to produce ROS (Lee et al., 1999), and, like c-Myc, activated ras can also induce DNA damage (Denko et al., 1994) and senescence (Serrano et al., 1997). These data raise the possibility that other activators of the MAPK pathway, such as receptor tyrosine kinases, and other proteins frequently overexpressed in human cancers, may generate excess ROS. Since normal mitogenic signaling also produces low amounts of ROS (Irani et al., 1997), we infer that cells have evolved mechanisms to limit DNA damage induction under such conditions. By contrast, oncogene activation may generate either higher levels of ROS or result in its induction for longer periods. An inability to buffer the effects of increased ROS resulting from persistently activated oncogenes may lead to DNA damage in certain cell types.

c-Myc Overexpression Compromises the DNA Damage Response

We found that c-Myc overexpression compromised the p53-dependent cell cycle arrest response triggered by DNA damage and promoted the entry of numerous cells into the cycle. This is compatible with other studies showing that c-Myc overexpression can override p53- and pRb-associated growth arrest following their ectopic expression or expression of G1 cyclin-dependent kinase inhibitors including p15, p16, p18, p19, and p27 (e.g., see Alevizopoulos et al., 1997). Our studies additionally demonstrate that c-Myc overexpression can compromise the diverse cell cycle arrest programs activated by DNA damage. Abrogation of DNA damage-induced G1/S arrest by c-Myc has also recently been observed in human epithelial cells (Sheen and Dickson, 2002). These observations raise the possibility that c-Myc overexpression in tumors may reduce the effectiveness of radiation and chemotherapies whose efficacy derives from induction of a DNA damage response.

Oncogene-Induced Genomic Instability during Tumor Progression

An implication of the data presented here is that mutations that arise during cancer progression can act as endogenous inducers of genetic instability as proposed by Nowell (1976). Mutations that activate c-Myc, including amplification, translocation, activation of β- or γ-catenin through WNT signaling or deletion of *apc* (Kolligs et al., 2000), or components of the MAPK pathway (Irani et al., 1997; Lee et al., 1999) may generate sufficient ROS to induce DNA damage. Deregulation of other pathways may also override p53-dependent arrest responses and drive some cells with DNA damage into cycle. Consistent with this, a recent study showed that activation of the MAPK pathway by raf can blunt p53 function by inducing the p53 ubiquitin ligase MDM2 (Ries et al., 2000), and other studies show that AKT activation leads

to MDM2-dependent p53 degradation (Mayo and Donner, 2001; Zhou et al., 2001). While most cells that enter the cell cycle with DNA damage would be expected to die as a result of lethal chromosome damage or mitotic catastrophe, rare survivors with additional mutations that improve survival, such as those that completely disable the p53 pathway, would be expected to arise. This model is consistent with the frequent emergence of p53-deficient clones in tumors expressing high levels of c-Myc (Eischen et al., 1999) or WNT (Jones et al., 1997). Complete loss of the p53 pathway would then create a permissive environment in which cells with DNA damage would be able to cycle, thereby fueling the genesis of additional variants. This provides a view in which oncogene activation both drives cellular proliferation and induces chromosomal abnormalities. We suggest that the aberrant chromosomes detected in biopsy samples of tumors with activated oncogenes and a defective p53 pathway are evidence of continuing genomic plasticity rather than relics of an early genome destabilizing event.

Experimental Procedures

Cell Culture

NHF containing the c-MycER (NHF-MycER) construct or the retroviral backbone (NHF-BABE), their respective HPV16 E6 infected derivatives, and Rat1aMycER were provided by Dr. Dean Felsher (Stanford University). Cells were cultured in DMEM lacking phenol red, supplemented with 10% (0.05% for serum deprivation) dialyzed FBS, L-glutamine, penicillin/streptomycin, Fungizone, and puromycin (1–2 μg/ml) and maintained in 7% CO_2 at 37°C. Cells were serum deprived at approximately 50% confluence, and c-MycER was activated by adding estrogen (E2, 2–10 μM) or 4-hydroxy-tamoxifen (OHT, 0.5–1 μM). Prior to all experiments, immunofluorescence and Western blotting were performed to ensure high-level expression and robust activation of the c-MycER construct. Continuous selection is required to maintain sufficient Myc levels to induce ROS. For cytological fluorescence assays, cells were grown on coverslips in six-well culture dishes. Serum-deprived cells were treated with NAC or BSO at final concentrations specified in the text.

Chemicals and γ Irradiation

BrdU and FITC-conjugated monoclonal anti-BrdU were obtained from PharMingen (San Diego, CA). Cells were γ irradiated at room temperature using a ^{60}Co γ irradiator (Gammabeam 150-C) at a distance of 35 cm at approximately 3.8 Gy/min. All other chemicals were obtained from Sigma (St. Louis, MO).

Cell Cycle Analyses

Cells were treated as specified in the text and pulsed with BrdU for 1 hr prior to processing as previously described (Linke et al., 1996). Cells were analyzed by flow cytometry using a Beckton-Dickinson FACScan equipped with a single 488 nm argon laser. G0/G1, S, and G2/M fractions were quantified using CELLQuest (Beckton-Dickinson, San Jose, CA). Representative examples of multiple experiments are shown.

TUNEL Assay and Immunocytochemistry

For TUNEL analyses, cells were briefly rinsed with PBS and fixed in 4% formaldehyde/PBS for 10 min, followed by four 5 min washes in PBS prior to processing or storage in PBS at 4°C. TUNEL using the In situ Cell Death Detection Kit (Boehringer Mannheim, Indianapolis, IN) was performed according to the manufacturer's specification with minor modifications as follows. Fixed cells were permeabilized in 0.1% Triton-X 100/PBS for 5 min. The cells were then washed in PBS and blocked in 0.1% BSA/0.1% TX-100/PBS at 37°C for 20 min prior to incubation with TUNEL reaction buffer in a light-safe, humidified chamber for 45 min at 37°C. Subsequent immunolocalization was performed using various primary antibodies diluted in 1%BSA/PBS-TX: pAb anti-hMre11, 1:200 (John Petrini, Madison, WI); pAb anti-p95, 1:200 (JP); pAb gX I-9 antiphosphorylated H2AX, 1:100 (Bill Bonner, NIH, Bethesda, MD), mAb anti-p53 (DO-1), 1:100 (Santa Cruz Biotechnology Inc., Santa Cruz, CA); mAb anti-BRCA1 (Ab-1), 1:100 (Calbiochem, San Diego CA), mAb anti-RPA-70 (Ab-1), 1:100 (Calbiochem). Immunolocalization of c-Myc was performed using Ab-3 (1:50, Santa Cruz Biotechnology Inc.), and cytoplasmic actin was stained with Texas Red-X phalloidin (Molecular Probes, Eugene, OR). Immunolocalization of cytochrome *c* was performed using polyclonal anti-cytochrome *c* (1:50, sc-7159, Santa Cruz, CA) and anti-rabbit conjugated to FITC (1:200, Jackson ImmunoResearch, PA). Coverslips were incubated with antibody in a humidified chamber at 37°C for 1 hr (cytochrome *c*, 3h). After washing, coverslips were incubated with fluorophore-conjugated secondary antibody (1:100) for 1 hr. Coverslips were mounted onto slides in Vectashield (Vector, Burlingame, CA) containing DAPI (1 μg/ml).

Immunofluorescence and Deconvolution Microscopy

Digital images of fluorescent nuclei spanning a z-series of 2–5 microns and taken every 0.2 microns were captured with an Olympus IX70 microscope (100× objective) equipped with a motorized stage and coupled to a digital CCD camera. Images of control and experimental cells were acquired using identical exposure times and stored using the Deltavision deconvolution computer software system (Silicon Graphics, Inc.; Applied Precision Inc., Issaquah, WA). Ideal exposure times for image acquisition from the DAPI and rhodamine channels were determined by the automated "Find Exposure" function of the operating software. TUNEL images were acquired by setting the FITC channel exposure to 5 s for each section. Captured images of the three wavelengths per viewing plane and spanning ten sections were deconvolved (ten cycles) and stacked into single volume images. Volume images were evaluated for signal and noise and uniformly adjusted to increase signal-to-noise ratio by adjusting contrast and brightness to resolve TUNEL foci. TUNEL foci in the three-color volume images were resolved by adjusting the FITC histogram signal cut-off to near maximal intensity in order to eliminate background haze and to resolve individual spots. Images were saved as TIFF files before digital transfer and compilation in Adobe Photoshop (Adobe Systems Inc., San Jose, CA).

ROS Assay and Quantitation

Cells were assayed for the generation of ROS using the fluorescence indicator of oxidative stress, dichlorofluorescein diacetate (DCFDA). Freshly made DCFDA (stock 6 mM in DMSO) was added directly to cell cultures (final concentration 2 μM) at 37°C for 25 min. Excess DCFDA was then removed with rinsing and a 5 min wash in serum starve medium at 37°C, and coverslips were wet-mounted onto slides. Fluorescence images from multiple fields of view were captured using a 20× objective and an FITC filter on a Zeiss Axioplan II microscope equipped with a Princeton Instruments CCD camera and operated using OpenLab software (Improvision, Coventry, England) at a designated exposure setting for all images. Captured grayscale digital images were false colored in Adobe Photoshop and quantitated for fluorescence intensity levels using OpenLab software. Relative mean fluorescence levels were obtained at a per cell basis for each digital image.

Immunoblot Analysis

Immunoblotting of whole-cell lysates was performed by procedures described previously (Sullivan et al., 1994). Monoclonal antibodies against c-Myc (Ab-3) (Calbiochem, San Diego, CA), BAG-1 (Dako Corporation, Carpinteria, CA), Rb (3C8) (Canji Inc., San Diego, CA), p53 (DO-1) (Santa Cruz Biotechnology Inc., Santa Cruz, CA), actin (Sigma, St. Louis, MO), and polyclonal antibodies against p27 (Santa Cruz Biotechnology Inc.) and phospho-Ser15 p53 (Cell Signaling Technology, MA) were used at final concentrations of 1–5 μg/ml. Polyclonal antibodies against Cyclin D1 (diluted 1:1000) were a gift from Tony Hunter (Salk Institute). Membranes were then washed and incubated with HRP-conjugated secondary antibodies (Amersham, Arlington Heights, IL) and detected using Pierce SuperSignal (Pierce, Rockford, IL). Densitometric analysis was performed using NIH image.

Colony Formation Assay

NHF-MycER and NHF-BABE cells were plated at 3000 cells per well in six-well tissue culture dishes and induced after culture as specified. Where specified, NAC was added for the final 24 hr of a 48 hr serum starvation. Fresh NAC and/or OHT was added to control and treated cells, in medium containing 10% or 0.05% dFBS, for 4 or 8 hr. Cells were then grown in media containing 10% dFBS for 6 days, washed in PBS, and fixed with 4% formaldehyde/PBS. Colonies were visualized after staining with crystal violet.

Preparation of RNA and Hybridization of Affymetrix Hu6800 GeneChip

Cultured cells were lysed and homogenized using Qia-shredder spin columns (Qiagen, Valencia, CA) and total RNA extracted using the RNeasy MiniKit (Qiagen). Preparation of labeled cRNA, hybridization to GeneChips, and scanning were performed essentially as described in Wodicka et al. (1997). The human Hu6800 GeneChip was used for all experiments (Affymetrix, Santa Clara, CA; http://www.affymetrix.com).

Analysis of GeneChip Hybridization Data

Hybridization data was analyzed using the Affymetrix GeneChip software, version 3.1 and an "in-house" Java-script, NfueGGo version 4.5 (D.J. Lockhart, personal communication). For further details, see Supplemental Data at http://www.molecule.org/cgi.content/full/9/5/1031/DC1.

RT-PCR

Cyclin D2 transcripts were amplified by PCR in the presence of primers specific for 18S rRNA using previously described methods (Welsh et al., 2001). PCR products were visualized on 2% agarose gels stained with ethidium bromide and images captured by a UVP laboratory Image Analysis System (UVP Inc., Upland, CA). Integrated optical densities (IOD) of the PCR products were determined using Labworks software (UVP Inc.) and the ratio of gene-specific to 18S IODs used to calculate fold induction.

Acknowledgments

We thank Dean Felsher (Stanford University) for providing NHF-MycER and NHF-BABE and HPV E6 derivatives and Rat1aMycER, John Petrini (University of Wisconsin) for antibodies against hMre11 and p95, Bill Bonner (NIH) for antibodies against phosphorylated H2AX, David Chambers and Kelly Hardwicke (Salk Institute) for their assistance in flow cytometry analyses, Sonu Dhar (Columbia University) for PCC analyses, Dr. Gretchen Jimenez (Salk Institute/Vical) for independent confirmation of several results, Lisa Sapinoso (GINRF) for excellent technical assistance, Dr Franck Toledo (Salk Institute) for comments on the manuscript, Dr. David J. Lockhart (GINRF) for advice and suggestions on analysis of the microarray data and for providing us with version 4.5 of the NfueGGo filtering software, and Ms. Ta'Neashia Morrell (Salk Institute) for administrative assistance. This work was supported by the California Research Program from the UC Regents (O.V.) and by a grant from the National Institutes of Health (G.M.W.).

Received: August 31, 2000
Revised: March 11, 2002

References

Agarwal, M.L., Agarwal, A., Taylor, W.R., and Stark, G.R. (1995). p53 controls both the G2/M and the G1 cell cycle checkpoints and mediates reversible growth arrest in human fibroblasts. Proc. Natl. Acad. Sci. USA *92*, 8493–8497.

Agarwal, M.L., Agarwal, A., Taylor, W.R., Chernova, O., Sharma, Y., and Stark, G.R. (1998). A p53-dependent S-phase checkpoint helps to protect cells from DNA damage in response to starvation for pyrimidine nucleotides. Proc. Natl. Acad. Sci. USA *95*, 14775–14780.

Alevizopoulos, K., Vlach, J., Hennecke, S., and Amati, B. (1997). Cyclin E and c-Myc promote cell proliferation in the presence of p16INK4a and of hypophosphorylated retinoblastoma family proteins. EMBO J. *16*, 5322–5333.

Artandi, S.E., Chang, S., Lee, S.L., Alson, S., Gottlieb, G.J., Chin, L., and DePinho, R.A. (2000). Telomere dysfunction promotes nonreciprocal translocations and epithelial cancers in mice. Nature *406*, 641–645.

Bates, S., Phillips, A.C., Clark, P.A., Stott, F., Peters, G.P., Ludwig, R.L., and Vousden, K.H. (1998). $p14^{ARF}$ links the tumour suppressors RB and p53. Nature *395*, 124–125.

Bell, D.W., Varley, J.M., Szydlo, T.E., Kang, D.H., Wahrer, D.C., Shannon, K.E., Lubratovich, M., Verselis, S.J., Isselbacher, K.J., Fraumeni, J.F., et al. (1999). Heterozygous germ line hCHK2 mutations in Li-Fraumeni syndrome. Science *286*, 2528–2531.

Chen, J.J., Silver, D., Cantor, S., Livingston, D.M., and Scully, R. (1999). BRCA1, BRCA2, and Rad51 operate in a common DNA damage response pathway. Cancer Res. *59*, 1752s–1756s.

Coller, H.A., Grandori, C., Tamayo, P., Colbert, T., Lander, E.S., Eisenman, R.N., and Golub, T.R. (2000). Expression analysis with oligonucleotide microarrays reveals that MYC regulates genes involved in growth, cell cycle, signaling, and adhesion. Proc. Natl. Acad. Sci. USA *97*, 3260–3265.

Dang, C.V. (1999). c-Myc target genes involved in cell growth, apoptosis, and metabolism. Mol. Cell. Biol. *19*, 1–11.

Denko, N.C., Giaccia, A.J., Stringer, J.R., and Stambrook, P.J. (1994). The human Ha-ras oncogene induces genomic instability in murine fibroblasts within one cell cycle. Proc. Natl. Acad. Sci. USA *91*, 5124–5128.

Di Leonardo, A., Linke, S.P., Clarkin, K., and Wahl, G.M. (1994). DNA damage triggers a prolonged p53-dependent G1 arrest and long-term induction of Cip1 in normal human fibroblasts. Genes Dev. *8*, 2540–2551.

Duelli, D.M., and Lazebnik, Y.A. (2000). Primary cells suppress oncogene-dependent apoptosis. Nat. Cell Biol. *2*, 859–862.

Eischen, C.M., Weber, J.D., Roussel, M.F., Sherr, C.J., and Cleveland, J.L. (1999). Disruption of the ARF-Mdm2-p53 tumor suppressor pathway in Myc-induced lymphomagenesis. Genes Dev. *13*, 2658–2669.

Eisen, M.B., Spellman, P.T., Brown, P.O., and Botstein, D. (1998). Cluster analysis and display of genome-wide expression patterns. Proc. Natl. Acad. Sci. USA *95*, 14863–14868.

el-Deiry, W.S., Kern, S.E., Pietenpol, J.A., Kinzler, K.W., and Vogelstein, B. (1992). Definition of a consensus binding site for p53. Nat. Genet. *1*, 45–49.

Evan, G.I., Wyllie, A.H., Gilbert, C.S., Littlewood, T.D., Land, H., Brooks, M., Waters, C.M., Penn, L.Z., and Hancock, D.C. (1992). Induction of apoptosis in fibroblasts by c-Myc protein. Cell *69*, 119–128.

Factor, V.M., Kiss, A., Wlitach, J.T., Wirth, P.J., and Thorgeirsson, S.S. (1998). Disruption of redox homeostasis in the transforming growth factor-alpha/c-Myc trangenic mouse model of accelerated hepatocarcinogenesis. J. Biol. Chem. *273*, 15846–15853.

Felsher, D.W., and Bishop, J.M. (1999). Transient excess of MYC activity can elicit genomic instability and tumorigenesis. Proc. Natl. Acad. Sci. USA *96*, 3940–3944.

Fishel, R., Lescoe, M.K., Rao, M.R., Copeland, N.G., Jenkins, N.A., Garber, J., Kane, M., and Kolodner, R. (1993). The human mutator gene homolog MSH2 and its association with hereditary nonpolyposis colon cancer. Cell *75*, 1027–1038.

Frank, S.R., Schroeder, M., Fernandez, P., Taubert, S., and Amati, B. (2001). Binding of c-Myc to chromatin mediates mitogen-induced acetylation of histone H4 and gene activation. Genes Dev. *15*, 2069–2082.

Gavrieli, Y., Sherman, Y., and Ben-Sasson, S.A. (1992). Identification of programmed cell death in situ via specific labeling of nuclear DNA fragmentation. J. Cell Biol. *119*, 493–501.

Graeber, T.G., Peterson, J.F., Tsai, M., Monica, K., Fornace, A.J., Jr., and Giaccia, A.J. (1994). Hypoxia induces accumulation of p53 protein, but activation of a G1- phase checkpoint by low-oxygen conditions is independent of p53 status. Mol. Cell. Biol. *14*, 6264–6277.

Harvey, M., McArthur, M.J., Montgomery, C.A., Jr., Bradley, A., and

Donehower, L.A. (1993). Genetic background alters the spectrum of tumors that develop in p53-deficient mice. FASEB J. *7*, 938–943.

Hermeking, H., and Eick, D. (1994). Mediation of c-Myc-induced apoptosis by p53. Science *265*, 2091–2093.

Hermeking, H., Funk, J.O., Reichert, M., Ellwart, J.W., and Eick, D. (1995). Abrogation of p53-induced cell cycle arrest by c-Myc: evidence for an inhibitor of p21/WAF1/CIP1/SDI1. Oncogene *11*, 1409–1415.

Hermeking, H., Lengauer, C., Polyak, K., He, T.C., Zhang, L., Thiagalingam, S., Kinzler, K.W., and Vogelstein, B. (1997). 14–3-3 σ is a p53-regulated inhibitor of G2/M progression. Mol. Cell *1*, 3–11.

Hollstein, M., Sidransky, D., Vogelstein, B., and Harris, C.C. (1991). p53 mutations in human cancers. Science *253*, 49–53.

Hwang, B.J., Ford, J.M., Hanawalt, P.C., and Chu, G. (1999). Expression of the p48 xeroderma pigmentosum gene is p53-dependent and is involved in global genomic repair. Proc. Natl. Acad. Sci. USA *96*, 424–428.

Irani, K., Xia, Y., Zweier, J.L., Sollott, S.J., Der, C.J., Fearon, E.R., Sundaresan, M., Finkel, T., and Goldschmidt-Clermont, P.J. (1997). Mitogenic signaling mediated by oxidants in Ras-transformed fibroblasts. Science *275*, 1649–1652.

Jimenez, G., Nister, M., Beeche, M., Barcarse, E., O'Gorman, S., and Wahl, G.M. (2000). A transactivation-deficient mouse model provides insights into p53 regulation and function. Nat. Genet. *26*, 37–43.

Johnson, R.T., and Rao, P.N. (1970). Mammalian cell fusion: induction of premature chromosome condensation in interphase nuclei. Nature *226*, 717–722.

Jones, J.M., Attardi, L., Godley, L.A., Laucirica, R., Medina, D., Jacks, T., Varmus, H.E., and Donehower, L.A. (1997). Absence of p53 in a mouse mammary tumor model promotes tumor cell proliferation without affecting apoptosis. Cell Growth Differ. *8*, 829–838.

Juin, P., Hueber, A.-O., Littlewood, T., and Evan, G. (1999). c-Myc-mediated sensitization to apoptosis is mediated through cytochrome *c* release. Genes Dev. *13*, 1367–1381.

Kamijo, T., Zindy, F., Roussel, M.F., Quelle, D.E., Downing, J.R., Ashmun, R.A., Grosveld, G., and Sherr, C.J. (1997). Tumor suppression at the mouse INK4a locus mediated by the alternative reading frame product p19ARF. Cell *91*, 649–659.

Kastan, M.B., Onyekwere, O., Sidransky, D., Vogelstein, B., and Craig, R.W. (1991). Participation of p53 protein in the cellular response to DNA damage. Cancer Res. *51*, 6304–6311.

Kastan, M.B., Zhan, Q., el-Deiry, W.S., Carrier, F., Jacks, T., Walsh, W.V., Plunkett, B.S., Vogelstein, B., and Fornace, A.J., Jr. (1992). A mammalian cell cycle checkpoint pathway utilizing p53 and GADD45 is defective in ataxia-telangiectasia. Cell *71*, 587–597.

Kern, S.E., Kinzler, K.W., Bruskin, A., Jarosz, D., Friedman, P., Prives, C., and Vogelstein, B. (1991). Identification of p53 as a sequence-specific DNA-binding protein. Science *252*, 1708–1711.

Ko, L.J., and Prives, C. (1996). p53: puzzle and paradigm. Genes Dev. *10*, 1054–1072.

Kolligs, F.T., Kolligs, B., Hajra, K.M., Hu, G., Tani, M., Cho, K.R., and Fearon, E.R. (2000). gamma-Catenin is regulated by the APC tumor suppressor and its oncogenic activity is distinct from that of beta-catenin. Genes Dev. *14*, 1319–1331.

Leach, F.S., Nicolaides, N.C., Papadopoulos, N., Liu, B., Jen, J., Parsons, R., Peltomaki, P., Sistonen, P., Aaltonen, L.A., Nystrom-Lahti, M., et al. (1993). Mutations of a mutS homolog in hereditary nonpolyposis colorectal cancer. Cell *75*, 1215–1225.

Lee, A.C., Fenster, B.E., Ito, H., Takeda, K., Bae, N.S., Hirai, T., Yu, Z.X., Ferrans, V.J., Howard, B.H., and Finkel, T. (1999). Ras proteins induce senescence by altering the intracellular levels of reactive oxygen species. J. Biol. Chem. *274*, 7936–7940.

Lee, T.C., Li, L., Philipson, L., and Ziff, E.B. (1997). Myc represses transcription of the growth arrest gene gas1. Proc. Natl. Acad. Sci. USA *94*, 12886–12891.

Li, T.K., Chen, A.Y., Yu, C., Mao, Y., Wang, H., and Liu, L.F. (1999). Activation of topoisomerase II-mediated excision of chromosomal DNA loops during oxidative stress. Genes Dev. *13*, 1553–1560.

Li, L.Y., Luo, X., and Wang, X. (2001). Endonuclease G is an apoptotic DNase when released from mitochondria. Nature *412*, 95–99.

Lin, W.C., Lin, F.C., and Nevins, J.R. (2001). Selective induction of E2F1 in response to DNA damage, mediated by ATM-dependent phosphorylation. Genes Dev. *15*, 1833–1844.

Linke, S.P., Clarkin, K.C., Di Leonardo, A., Tsou, A., and Wahl, G.M. (1996). A reversible, p53-dependent G0/G1 cell cycle arrest induced by ribonucleotide depletion in the absence of detectable DNA damage. Genes Dev. *10*, 934–947.

Livingstone, L.R., White, A., Sprouse, J., Livanos, E., Jacks, T., and Tlsty, T.D. (1992). Altered cell cycle arrest and gene amplification potential accompany loss of wild-type p53. Cell *70*, 923–935.

Loeb, L.A. (2001). A mutator phenotype in cancer. Cancer Res. *61*, 3230–3239.

Mai, S., Fluri, M., Siwarski, D., and Huppi, K. (1996). Genomic instability in MycER-activated Rat1A-MycER cells. Chromosome Res. *4*, 365–371.

Mayo, L.D., and Donner, D.B. (2001). A phosphpatidylinositol 3-kinase/Akt pathway promotes translocation of Mdm2 from the cytoplasm to the nucleus. Proc. Natl. Acad. Sci. USA *98*, 11598–11603.

McCarthy, N.J., Whyte, M.K., Gilbert, C.S., and Evan, G.I. (1997). Inhibition of Ced-3/ICE-related proteases does not prevent cell death induced by oncogenes, DNA damage, or the Bcl-2 homologue Bak. J. Cell Biol. *136*, 215–227.

Meister, A. (1983). Selective modification of glutathione metabolism. Science *220*, 472–477.

Nelms, B.E., Maser, R.S., MacKay, J.F., Lagally, M.G., and Petrini, J.H. (1998). In situ visualization of DNA double-strand break repair in human fibroblasts. Science *280*, 590–592.

Nowell, P.C. (1976). The clonal evolution of tumor cell populations. Science *194*, 23–28.

O'Hagan, R.C., Schreiber-Agus, N., Chen, K., David, G., Engelman, J.A., Schwab, R., Alland, L., Thomson, C., Ronning, D.R., Sacchettini, J.C., et al. (2000). Gene-target recognition among members of the myc superfamily and implications for oncogenesis. Nat. Genet. *24*, 113–119.

Ohba, M., Shibanuma, M., Kuroki, T., and Nose, K. (1994). Production of hydrogen peroxide by transforming growth factor-beta 1 and its involvement in induction of egr-1 in mouse osteoblastic cells. J. Cell Biol. *126*, 1079–1088.

Packham, G., and Cleveland, J.L. (1994). Ornithine decarboxylase is a mediator of c-Myc-induced apoptosis. Mol. Cell. Biol. *14*, 5741–5747.

Pandita, T.K., and Hittelman, W.N. (1992). The contribution of DNA and chromosome repair deficiencies to the radiosensitivity of ataxia-telangiectasia. Radiat. Res. *131*, 214–223.

Pandita, T.K., Gregoire, V., Dhingra, K., and Hittelman, W.N. (1994). Effect of chromosome size on aberration levels caused by gamma radiation as detected by fluorescence in situ hybridization. Cytogenet. Cell Genet. *67*, 94–101.

Paulson, T.G., Almasan, A., Brody, L.L., and Wahl, G.M. (1998). Gene amplification in a p53-deficient cell line requires cell cycle progression under conditions that generate DNA breakage. Mol. Cell. Biol. *18*, 3089–3100.

Polyak, K., Xia, Y., Zweier, J.L., Kinzler, K.W., and Vogelstein, B. (1997). A model for p53-induced apoptosis. Nature *389*, 300–305.

Poupon, M.F., Smith, K.A., Chernova, O.B., Gilbert, C., and Stark, G.R. (1996). Inefficient growth arrest in response to dNTP starvation stimulates gene amplification through bridge-breakage-fusion cycles. Mol. Biol. Cell *7*, 345–354.

Ries, S., Biederer, C., Woods, D., Shifman, O., Shrasawa, S., Sasazuki, T., McMahon, M., Oren, M., and McCormick, F. (2000). Opposing effects of ras on p53: transcriptional activation of mdm2 and induction of p19ARF. Cell *103*, 321–330.

Robles, S.J., and Adami, G.R. (1998). Agents that cause DNA double strand breaks lead to p16INK4a enrichment and the premature senescence of normal fibroblasts. Oncogene *16*, 1113–1123.

Rogakou, E.P., Pilch, D.R., Orr, A.H., Ivanova, V.S., and Bonner,

W.M. (1998). DNA double-stranded breaks induce histone H2AX phosphorylation on serine 139. J. Biol. Chem. *273*, 5858–5868.

Rotman, G., and Shiloh, Y. (1999). ATM: a mediator of multiple responses to genotoxic stress. Oncogene *18*, 6135–6144.

Sah, V.P., Attardi, L.D., Mulligan, G.J., Williams, B.O., Bronson, R.T., and Jacks, T. (1995). A subset of p53-deficient embryos exhibit exencephaly. Nat. Genet. *10*, 175–180.

Sheen, J.H., and Dickson, R.B. (2002). Overexpression of c-Myc alters G(1)/S arrest following ionizing radiation. Mol. Cell. Biol. *22*, 1819–1833.

Sherr, C.J. (1998). Tumor surveillance via the ARF-p53 pathway. Genes Dev. *12*, 2984–2991.

Sherr, C.J., and Weber, J.D. (2000). The ARF/p53 pathway. Curr. Opin. Genet. Dev. *10*, 94–99.

Serrano, M., Lin, A.W., McCurrach, M.E., Beach, D., and Lowe, S.W. (1997). Oncogenic ras provokes premature cell senescence associated with accumulation of p53 and p16INK4a. Cell *88*, 593–602.

Sullivan, K.F., Hechenberger, M., and Masri, K. (1994). Human CENP-A contains a histone H3 related histone fold domain that is required for targeting to the centromere. J. Cell Biol. *127*, 581–592.

Thorgeirsson, S.S., Factor, V.M., and Snyderwine, E.G. (2000). Transgenic mouse models in carcinogenesis research and testing. Toxicol. Lett. *112–113*, 553–555.

Wahl, G.M., and Carr, A.M. (2001). The evolution of diverse biological responses to DNA damage: insights from yeast and p53. Nat. Cell Biol. *3*, E277–E286.

Wahl, G.M., Linke, S.P., Paulson, T.G., and Huang, L.C. (1997). Maintaining genetic stability through TP53 mediated checkpoint control. Cancer Surv. *29*, 183–219.

Ward, J.F. (1990). The yield of DNA double-strand breaks produced intracellularly by ionizing radiation: a review. Int. J. Radiat. Biol. *57*, 1141–1150.

Welsh, J.B., Zarrinkar, P.P., Sapinoso, L.M., Kern, S.G., Behling, C.A., Monk, B.J., Lockhart, D.J., Burger, R.A., and Hampton, G.M. (2001). Analysis of gene expression profiles in normal and neoplastic ovarian tissue samples identifies candidate molecular markers of epithelial ovarian cancer. Proc. Natl. Acad. Sci. USA *98*, 1176–1181.

Wodicka, L., Dong, H., Mittmann, M., Ho, M.H., and Lockhart, D.J. (1997). Genome-wide expression monitoring in Saccharomyces cerevisiae. Nat. Biotechnol. *13*, 1359–1367.

Yin, Y., Tainsky, M.A., Bischoff, F.Z., Strong, L.C., and Wahl, G.M. (1992). Wild-type p53 restores cell cycle control and inhibits gene amplification in cells with mutant p53 alleles. Cell *70*, 937–948.

Zhou, B.P., Liao, Y., Xia, W., Zou, Y., Spohn, B., and Huang, M.C. (2001). HER-2/neu induces p53 ubiquitination via Akt-mediated MDM2 phosphorylation. Nat. Cell Biol. *3*, 973–982.

Zindy, F., Eischen, C.M., Randle, D.H., Kamijo, T., Cleveland, J.L., Sherr, C.J., and Roussel, M.F. (1998). Myc signaling via the ARF tumor suppressor regulates p53-dependent apoptosis and immortalization. Genes Dev. *12*, 2424–2433.